Slow Motion Analysis of Protein Folding Intermediates within Wet Silica Gels[†]

Naoya Shibayama*

Department of Physiology, Division of Biophysics, Jichi Medical University, 3311-1 Yakushiji, Shimotsuke, Tochigi 329-0498, Japan

Received November 8, 2007; Revised Manuscript Received March 27, 2008

ABSTRACT: Resolving the complete folding pathway of a protein is a major challenge to conventional experimental methods because of the rapidity and complexity of folding. Here, we show that entrapment of the protein cytochrome *c* in wet, optically transparent, porous silica gel matrices has enabled a dramatic expansion, to days or weeks, of the folding time, allowing direct observation of the entire folding pathway using a combination of three spectroscopic techniques, far-ultraviolet circular dichroism, tryptophan fluorescence, and Soret absorption spectroscopy. During refolding in silica gels, collapse and helix formation occur in a stepwise manner, as observed in aqueous solution. Analysis of kinetics and transient spectra indeed reveals a sequence of four distinct intermediates with progressively increasing degrees of folding, two of which closely resemble those previously characterized in solution, namely, the early collapsed and the molten globule intermediates. The other two are the precollapsed and pre-molten globule intermediates that may escape detection by conventional kinetic methods. Interestingly, varying the strength of the gel network has a dramatic effect on the folding time, but no significant effect on the structural features of each folding intermediate, indicating that the interaction between the protein and gel matrix has no measurable effect on the folding pathway. These results better define the major pathway of cytochrome *c* folding. In addition, in this paper we present the results of the application of this method to a simple, apparent two-state folder ubiquitin, helping to interpret the results for cytochrome *c*.

Protein folding is a collective self-organization process that occurs over a wide range of time and space scales. Important folding events, including both chain collapse and secondary structure formation, occur on a microsecond time scale, which cannot be easily accessed by conventional mixing techniques (*1*). Although recent progress in laser temperature jump and other laser-based techniques has allowed us to study the early stages of protein folding with a time resolution down to tens of nanoseconds (*2–4*), these approaches can be applied only to certain proteins that either undergo cold denaturation (*2*) or have photosensitive chromophores (*3, 4*). Furthermore, another problem is the lack of good spectroscopic experimental techniques and designs that can be performed in a kinetic mode and yield detailed structural information about short-lived intermediates along the folding pathways. Here, we demonstrate a method by which the entire folding processes of proteins can be dramatically slowed and monitored directly with a combination of spectroscopic techniques. We have entrapped cytochrome *c* (cyt *c*)[1] in wet, optically transparent, porous silica gel matrices under mild sol−gel conditions such that the protein molecules are fully solvated and retain their spectroscopic properties in solution (*5–9*). The method has been shown to be a promising strategy for characterization of various dynamics and nonequilibrium conformations of solvated proteins by decelerating the large-scale motions (*6–13*). Hence, by applying this method, we should be able to slow the folding reactions of proteins with minimal perturbation to their folding pathways.

Horse cyt *c* is a small single-domain protein with 104 amino acids, whose folding process has been extensively studied with respect to its mechanism and intermediates (*14–19*). It has a heme group that is covalently bound to Cys14 and Cys17. Native state cyt *c* contains three major helices (i.e., N-terminal, C-terminal, and 60s helices) and two minor helical elements connected by loops, and its heme group is axially coordinated with the proximal His18 and Met80. Acidification of solutions of oxidized cyt *c* in the absence of added salt produces a cooperative transition having an apparent p*K* of 2.5 involving both the gross unfolding of the molecule (*20*) and the replacement of the two native axial heme ligands with a single solvent water molecule, leading to a five-coordinate state (*19*). In this study, we focus on the refolding of oxidized horse cyt *c*, starting from the low-salt acid-unfolded state at pH 1.8 to the native state at pH 4.7, because these acidic conditions prevent non-native histidine (His26/33)−heme ligation that complicates the folding pathway of cyt *c* (*15, 16, 19*).

To better interpret the results obtained for cyt *c* in wet silica gels, we further apply this method to study the folding of a simple model protein, bovine ubiquitin, that folds in an apparent two-state manner when not entrapped in silica gels (*21–23*). Ubiquitin is a 76-residue small protein without any cysteines, metal ions, or cofactors that might complicate

[†] This work was supported by Grant 17570135 from the Japanese Ministry of Education, Science, Sports, and Culture.

* To whom correspondence should be addressed: Department of Physiology, Division of Biophysics, Jichi Medical University, 3311-1 Yakushiji, Shimotsuke, Tochigi 329-0498, Japan. Telephone: +81-285-58-7308. Fax: +81-285-40-6294. E-mail: shibayam@jichi.ac.jp.

[1] Abbreviations: cyt *c*, cytochrome *c*; GuHCl, guanidinium hydrochloride; UV, ultraviolet; CD, circular dichroism; NATA, *N*-acetyltryptophanamide.

10.1021/bi8003582 CCC: $40.75
Published on Web 05/01/2008

the mechanism of protein folding. Native state ubiquitin has a globular structure consisting of a five-stranded β-sheet, a four-turn α-helix, and seven turns (*24*). Although the original studies on a fluorescent F45W mutant suggested that a stable intermediate is formed during refolding on the basis of significant curvature in the chevron plot at low concentrations of denaturant (*25*), recent experiments show that such non-two-state behavior can result from the transient aggregation of the hydrophobic (F45W) mutant (*23*), and no intermediate state is significantly populated during the refolding of ubiquitin (*22, 23*). Moreover, and importantly, several lines of evidence suggest that ubiquitin may fold through an on-pathway high-energy intermediate, which is normally unstable but can be stabilized by mutations and/or changes in experimental conditions (*23, 26*). Therefore, ubiquitin is an interesting model system for addressing the questions of how the gel matrix affects the simple folding behavior of a two-state protein, and whether our approach is able to capture such "hidden" folding intermediates. To address these issues, we characterize the refolding of GuHCl-denatured ubiquitin in silica gels on the basis of far-UV CD measurements. Then, the results are discussed with those for cyt *c* folding in silica gels.

EXPERIMENTAL PROCEDURES

Sol−Gel Entrapment, Unfolding, and Refolding of Cyt c. The silica sol was synthesized from tetramethylorthosilicate (Tokyo Kasei) as described previously (*5*). Oxidized horse cyt *c* (Sigma) was entrapped in wet silica gels that were prepared either as thin (∼0.02 mm) films for measuring the early folding kinetics or as sheets 0.1 mm in thickness for the measurement on the longer time region. The detailed procedures are given below.

To prepare a thin (∼0.02 mm) silica gel film, 0.01 mL of ice-cooled, silica sol was mixed with an equal volume of an ice-cooled, stock solution of 0.81 mM oxidized horse cyt *c* in 0.05 M potassium phosphate buffer (pH 7.1). Immediately after the solution had been mixed, 0.0075 mL of the mixture was coated as a thin layer [10 mm × ∼38 mm × ∼0.02 mm (thickness)] on a single optical window in a sealable rectangular quartz cuvette (1 cm path length), which had been pretreated with 4 N KOH for 30 min to maximize the number of surface silanol groups. Another optical window in the same cuvette was coated with 0.1 mL of silica gel of the same composition, but without protein, to keep the vapor pressure sufficiently high to prevent drying of the sample. Samples were allowed to stand at 4 °C to be gelled. Twenty minutes later, the gels were left to age at 20 °C for 3, 4, 16, or 72 h. Prior to the unfolding experiment, the aged samples were rinsed with excess distilled water to terminate the aging. Unfolding was carried out by immersing the samples in 0.02 M HCl (pH 1.8) at 20 °C. The attainment of unfolding equilibrium at pH 1.8 was ascertained by the stable value of the absorbance at 395 nm. Unfolding occurred within 30 min regardless of the aging time. Subsequently, refolding was initiated by immersion in 0.5 M potassium phosphate buffer (pH 4.7). After each refolding measurement, the absorption spectrum of the bathing solution was measured to determine the amount of protein that leaked from the gels. In all cases, the total amount of leakage during the refolding experiment was less than 3.5% of the original protein content. Note that the amount of leakage decreases with an increase in the sol−gel aging time.

To prepare a silica gel sheet 0.1 mm in thickness, 0.03 mL of ice-cooled, silica sol was mixed with an equal volume of an ice-cooled, stock solution of 0.48 mM oxidized horse cyt *c* in 0.05 M potassium phosphate buffer (pH 7.1). The mixture was layered on a quartz plate with a frame of 10 mm × 40 mm × 0.1 mm (depth) (Tosoh Quartz) at 4 °C, and then a Teflon plate was overlaid on the sample to form a gel sheet 0.1 mm in thickness. Samples were allowed to stand at 4 °C to be gelled. Twenty minutes later, the Teflon plate was gently removed and the gel adhering to the quartz plate was transferred into a 13 mm diameter sealed glass tube (10 cm in height) whose inner surface had been coated with a 0.2 mL volume of silica gel of the same composition but without protein. Aging, unfolding and refolding were carried out using the same procedures mentioned above for the thin (∼0.02 mm) film sample, except that the gel was covered with a quartz plate on and after the 1 min refolding period, to prevent protein leakage. During refolding, signals and spectra for three spectroscopic probes were detected sequentially on the same sample, covered with a quartz plate.

Native State Equilibrium Properties. The spectroscopic properties of native cyt *c* in silica gels were independently determined after equilibration of the aged samples (before unfolding) in 0.5 M potassium phosphate buffer (pH 4.7) for 1 week.

Sol−Gel Entrapment, Unfolding, and Refolding of Ubiquitin. Sol−gel entrapment of bovine ubiquitin (Sigma) was carried out using the same procedures described above for cyt *c* except with aging times of 16, 48, and 96 h. Unfolding was carried out by immersion in buffer [0.05 M potassium phosphate (pH 5.0)] containing 6.0 M GuHCl at 20 °C. The attainment of unfolding equilibrium was ascertained by the stable value of the CD at 222 nm. Unfolding occurred within 30 min regardless of the aging time. Subsequently, refolding was initiated by immersion in buffer without GuHCl at 20 °C.

Dead-Time Determination. To determine the pH response of the gel interior, we carried out a control experiment using a 70000 MW dextran conjugate of Oregon Green (Molecular Probes) as a pH indicator within the gels. The time required for equilibration of pH inside the silica gels after the pH of the bathing solution had changed from 1.8 to 4.7 was ∼40 s for a 0.1 mm silica gel sheet, and thus ∼1.5 s for a 0.02 mm silica gel thin film. This control experiment also indicated that the average pH within a 0.02 mm silica gel film reaches ∼4.5 approximately 1 s after immersion in the bathing solution at pH 4.7. Since cyt *c* folding can be inducible even at pH 4.5, we have followed the refolding of cyt *c* in ∼0.02 mm silica gel films from 1 s after the bathing solution had been changed. Note here that the response times of the pH inside the silica gels did not significantly vary with the sol−gel aging time.

To determine the time-dependent concentration change of GuHCl within silica gels after initiation of the refolding of ubiquitin, we carried out a control experiment using a protein-free 0.1 mm silica gel sheet which was initially equilibrated with buffer containing 6 M GuHCl. After immersion in the bathing solution without GuHCl, the decay of GuHCl absorbance at 207.5 nm was monitored as a function of time (Figure 3A, inset). We found that the GuHCl concentration

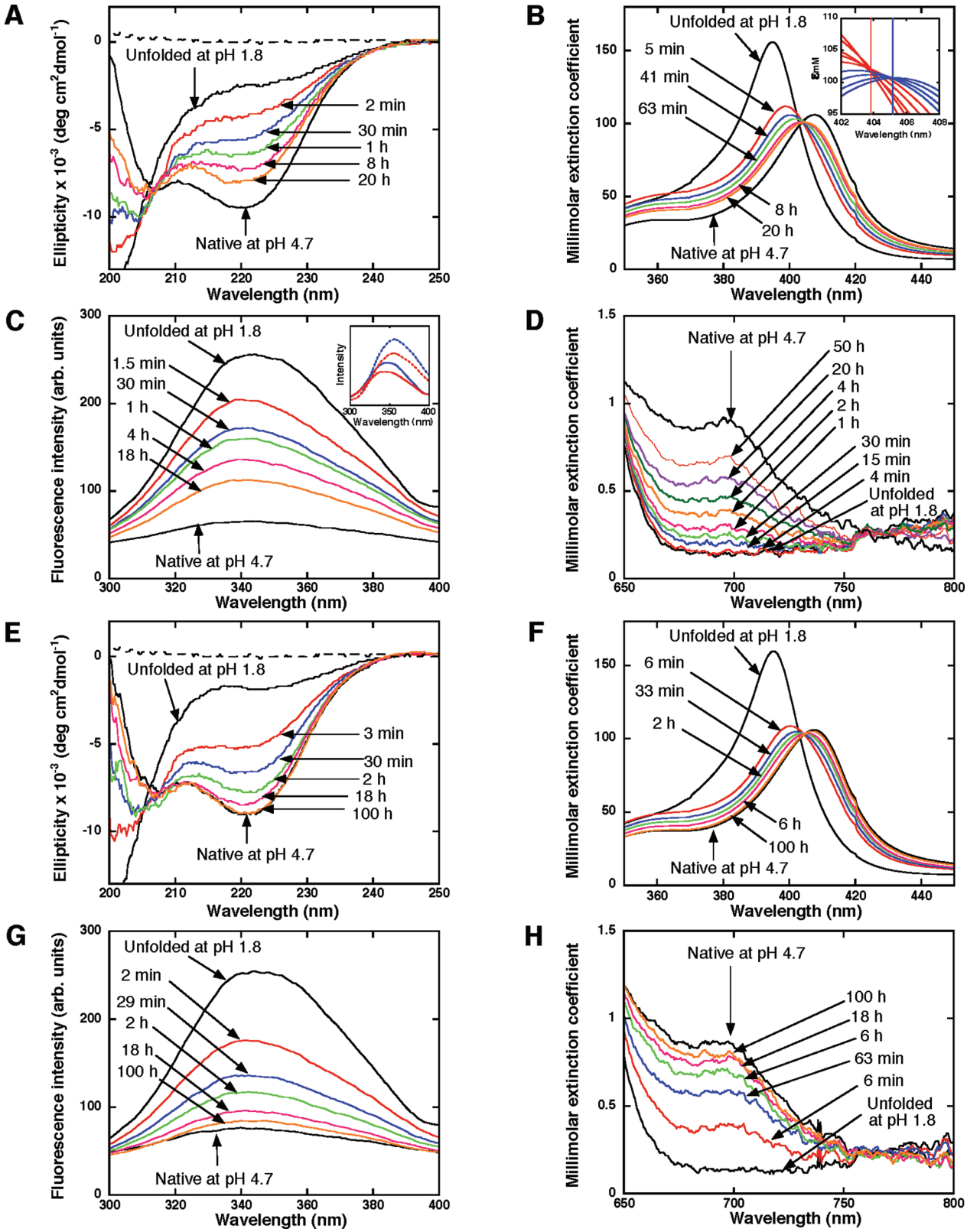

FIGURE 1: Representative transient far-UV CD, Soret absorption, Trp fluorescence, and charge-transfer band absorption spectra during the refolding of acid-denatured cyt *c* at pH 4.7 (20 °C) in wet silica gels 0.1 mm in thickness. (A) Far-UV CD spectra of cyt *c* in silica gels aged for 4 h. (B) Soret absorption spectra of cyt *c* in silica gels aged for 4 h. The inset shows the expanded view around 405 nm. The five initial spectra at time points 5, 15, 41, 63, and 123 min after the refolding are colored red, and the latter four spectra at 4, 8, 20, and 51 h are colored blue. (C) Trp fluorescence emission spectra of cyt *c* in silica gels aged for 4 h. The inset shows the fluorescence emission spectra of the initial acid-unfolded conformation (U) in the gel (solid red line) and in the free aqueous solution (solid blue line), in comparison with those of NATA at the same concentration in the gel (dashed red line) and in the aqueous solution (dashed blue line). (D) Charge-transfer band absorption spectra of cyt *c* in silica gels aged for 4 h. (E) Far-UV CD spectra of cyt *c* in silica gels aged for 3 h. (F) Soret absorption spectra of cyt *c* in silica gels aged for 3 h. (G) Trp fluorescence emission spectra of cyt *c* in silica gels aged for 3 h. (H) Charge-transfer band absorption spectra of cyt *c* in silica gels aged for 3 h. The dashed lines in panels A and E are a baseline CD spectrum of the wet silica gel without protein. For clarity, only five of the nine time points are displayed in each panel except for panel D. For panels D and H, we used a higher protein concentration of 1.1 mM (before sol−gel entrapment) to monitor the weak charge-transfer absorption band around 695 nm.

inside the 0.1 mm silica gels decreases from 6.0 to 0.58 M at 20 s and to less than 0.06 M at 120 s after the bathing solution is changed. On the basis of these findings, we have followed the refolding of ubiquitin in 0.1 mm silica gel sheets from 20 s after the bathing solution had been changed, and from 1 s when using 0.02 mm silica gel thin films.

Fluorescence Measurements. Front-face fluorometry was used to detect the fluorescence of cyt *c* in silica gel. Fluorescence measurements were carried out using a JASCO FP-6500 fluorometer, equipped with a thermostated cell holder. All the measurements were carried out at 20 °C. The exciting light makes an angle of 34° with the normal to the front face of the cell. For the kinetics measurements, the excitation wavelength was set at 280 nm, and the emission at 350 nm was observed through a long-path filter above 300 nm (Asahi Spectra, LU0300). The slit widths for excitation and emission light were set at 1 and 10 nm, respectively. The fluorescence kinetics at 350 nm were recorded every 1 s, with a 0.5 s response time during the initial 100 s. For longer kinetic experiments ($t > 100$ s), a computer-controlled shutter was used to minimize photobleaching. No significant photobleaching during the kinetic refolding experiment was indicated in the following control experiment. After the refolding experiment, each sample was re-unfolded by immersion in 0.02 M HCl (pH 1.8) at 20 °C. The emission of the sample was then measured during the same exposure time used for the refolding experiment. No significant photobleaching was found, confirming the negligible extent of photobleaching that occurred during the refolding experiment.

The Trp fluorescence emission spectra from 300 to 400 nm were collected every 0.5 nm with a 1 s response time, and a scan speed of 200 nm/min. An excitation wavelength of 290 nm was used to reduce the contribution of Tyr emission. For comparison, the fluorescence spectra of *N*-acetyltryptophanamide (NATA) at the same concentration in gel and in aqueous solution were measured under the same conditions.

CD Measurements. CD measurements were carried out using a JASCO J-600 spectropolarimeter equipped with a Peltier element for temperature control. All the measurements were carried out at 20 °C. The CD kinetics at 222 nm were recorded every 2 s with a 2 nm bandwidth and a 2 s response time. The CD spectra from 200 to 250 nm were collected every 0.2 nm with a 2 nm bandwidth, a 2 s response time, and a 20 nm/min scan speed.

Optical Absorption Measurements. Optical absorption measurements were carried out using a JASCO V-560 spectrophotometer equipped with a Peltier element for temperature control. All the measurements were carried out at 20 °C. For cyt *c*, the optical absorption kinetics at 395 nm were recorded every 1 s with a 2 nm bandwidth and a 0.25 s response time. The optical absorption spectra between 350 and 800 nm (for cyt *c*) or between 200 and 400 nm (for ubiquitin) were collected every 0.5 nm with a 2 nm bandwidth, a 1 s response time, and a 200 nm/min scan speed.

Data Fitting. For cyt *c* in thin silica gel films, the early folding kinetics in the time frame of 1−900 s (for the sample aged for 3 h), 1−2500 s (for the sample aged for 4 h), 1−7200 s (for the sample aged for 16 h), or 20−27000 s (for the sample aged for 72 h) were normalized with respect to the corresponding controls and were fitted to a stretched plus single exponential:

$$f(t) = a_0 - a_1 \exp[-(k_{1t})^{\beta}] - a_2 \exp(-k_2 t)$$

Although the amount of protein leakage during the refolding measurement was small in all cases for cyt *c* (<3.5% of the total protein), it was corrected by assuming the amount of leakage is proportional to the time. Then, the contributions of these early phases were subtracted from the slower data (obtained using 0.1 mm silica gel sheets), and the residuals were fitted to a double or single exponential.

For ubiquitin in thin silica gel films ~0.02 mm in thickness, the folding kinetics in the time frame of 6−20530 s (for the sample aged for 16 h), 6−20532 s (for the sample aged for 48 h), or 8−22200 s (for the sample aged for 96 h) were fitted to a double-exponential function. The amount of protein leakage within these time frames could not be detected by UV absorption measurements. For ubiquitin in silica gel sheets 0.1 mm in thickness, the transient CD spectra between 209 and 250 nm during refolding were globally fit to a three-state model (U → I → N) using SPECFIT (version 3.0.37, Spectrum Software Associates).

RESULTS

Experimental Designs. For cyt *c*, our experiments consist of the following steps: (i) entrapment of native state cyt *c* into silica gel matrices formed by hydrolysis and condensation of $Si(OCH_3)_4$ (tetramethylorthosilicate), (ii) aging, (iii) acid unfolding, and (iv) refolding. Four notable features of our silica gels are as follows. First, their high water content (a water mass fraction of 70%) allows studies of the folding process of proteins in an aqueous environment. Second, their high optical transparency allows various spectroscopic measurements. In this study, kinetics and transient spectra during refolding were followed with a combination of three spectroscopic techniques: far-UV CD to monitor the α-helices, the fluorescence of a single tryptophan (Trp59) to probe the molecular compactness, and Soret absorption spectroscopy to investigate the heme environment. Note that the Trp fluorescence intensity of cyt *c* directly reflects the average distance between the Trp59 and the heme group covalently attached to the protein, because in the compact native state the fluorescence of Trp59 is almost completely quenched by the heme through Förster energy transfer, but not so much in the extended unfolded state (*27*).

Third, their porosity allows nearly free diffusion of smaller molecules between the bathing solution and the proteins. Under our experimental conditions using thin (~0.02 mm thickness) silica gels, the aqueous gel environment can extend the folding time beyond the diffusion time of water and chemical solutes, thereby overcoming the dead-time problem. Finally, the degrees of conformational constraint on the entrapped proteins can be tuned by the time of "aging" that continues until a rinse with excess water. The initial wet gels are soft and have relatively large pores. Aging of the silica network over a period of hours to days promotes further condensation and strengthens the network (*28*). We therefore used four samples with different aging times of 3, 4, 16, and 72 h to systematically control the folding time of cyt *c* in wet silica gels.

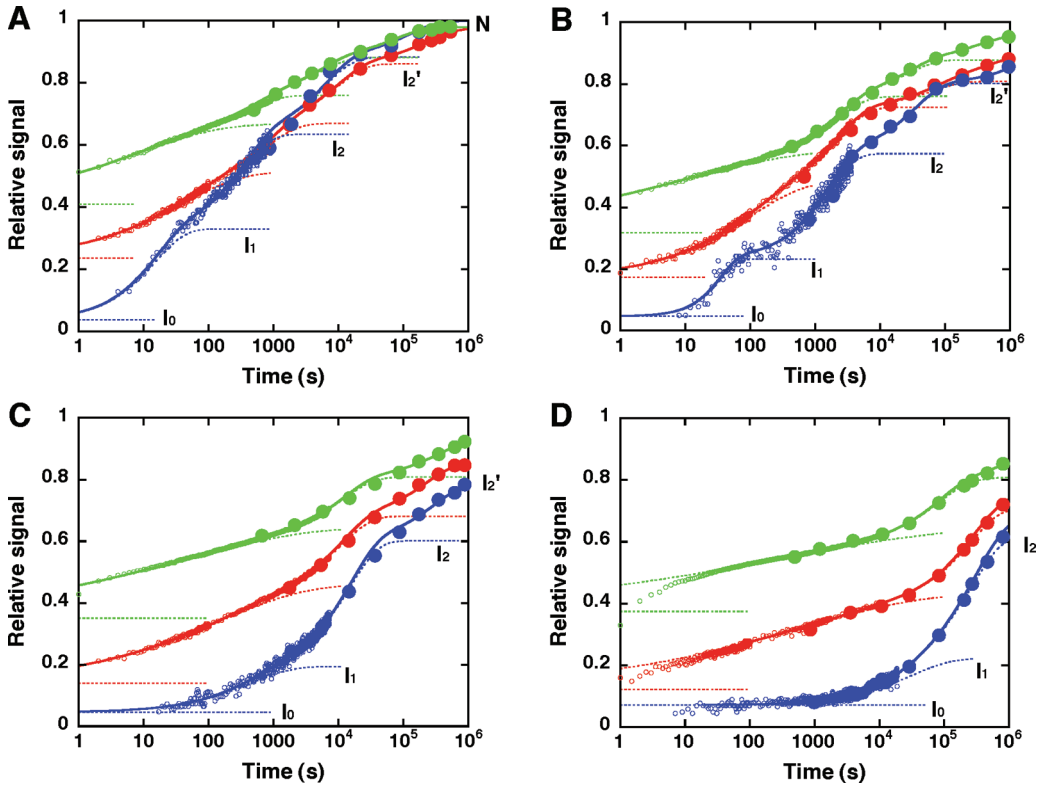

FIGURE 2: Normalized time courses of changes in signals of far-UV CD at 222 nm (blue), Trp59 fluorescence at 350 nm (red), and Soret absorption at 395 nm (green) during the refolding of acid-denatured cyt *c* at pH 4.7 (20 °C) in wet silica gels aged for (A) 3, (B) 4, (C) 16, and (D) 72 h, plotted on a logarithmic time scale. In each panel, the data obtained from ~0.02 mm silica gel thin films (small empty circles) and those from 0.1 mm silica gel sheets (large filled circles) are combined. Solid lines are the best fits for the entire kinetics (see Experimental Procedures), and dotted lines indicate each kinetic component.

In this work, we further apply this method to study the folding of ubiquitin. The following differences were noted between cyt *c* and ubiquitin experiments. First, to prevent leakage of the smaller ubiquitin molecule from silica gels, the longer aging times of 16, 48, and 96 h were used. Second, because ubiquitin is stable at acidic pHs, we chose a GuHCl concentration jump (instead of a pH jump) for ubiquitin unfolding and refolding. Third, ubiquitin contains no Trp residues and only one Tyr residue, so the refolding kinetics were monitored solely by far-UV CD.

Cyt c Unfolding. Each of the four aged samples described above was fully unfolded by immersion in 0.02 M HCl (pH 1.8) at 20 °C. At pH 1.8, the three spectroscopic probes showed that all the samples can attain, albeit slowly (typically 15−30 min), a very similar unfolded conformation (named U) that exhibits characteristics typical of an extended random coil structure with a five-coordinate high-spin heme as observed in low-pH solutions (see Figure 1). Note that the Trp fluorescence spectrum of U in gel has a slightly (21%) smaller intensity than that of U in aqueous solution (see the solid lines in the inset of Figure 1C). However, this difference may be due to a reduced quantum yield of tryptophan emission in the gel, and not due to a collapse caused by the spatial restriction of the gel matrix, since the fluorescence of free tryptophan (i.e., NATA) in the gel is decreased by a similar extent (22%) relative to that in the free aqueous solution (see the dashed lines in the inset of Figure 1C). Note also here that, although an extremely slow unfolding of cyt *c* in silica gels (typically 2−4 days) has recently been reported (*29*), the results cannot be compared directly because of the difference in the physical and chemical properties of silica gels.

Cyt c Refolding. Refolding was triggered by changing the bathing solution to 0.5 M potassium phosphate buffer (pH 4.7) at 20 °C. Refolding kinetics for each aged sample monitored by far-UV CD (222 nm), Trp59 fluorescence (350 nm), and Soret absorption (395 nm) are shown in each panel of Figure 2. As seen in Figure 2, cyt *c* in wet silica gels folds over a period of hours, days, weeks, or longer, depending on the aging time: the longer the aging time, the slower the folding. Analysis of kinetics and transient spectra during folding (Figures 1 and 2A,B) indicates that the faster two samples aged for 3 and 4 h fold through a sequential pathway with four common intermediates as described by the following scheme:

Scheme 1:

$$U \rightarrow I_0 \rightarrow I_1 \rightarrow I_2 \rightarrow I_2' \rightarrow N$$

Note that, as shown in panels C and D of Figure 2, although the refolding kinetics of the other samples (aged for 16 and 72 h) are too slow to reach N or even I_2' within the time frame investigated, the observed kinetics seem to be not inconsistent with Scheme 1.

The common folding pathway includes (i) rapid coordination of the proximal His18 residue to the heme iron, leading to the first intermediate, I_0, (ii) initial chain collapse to a compact intermediate, I_1, (iii) further collapse and helix formation to a pre-molten globule intermediate, I_2, (iv)

Table 1: Kinetic Parameters for the Refolding Kinetics of Acid-Denatured Cyt *c* at pH 4.7 (20 °C) in Wet Silica Gels Aged for 3, 4, 16, and 72 h[a]

		$U \rightarrow I_0$ (burst phase)	$I_0 \rightarrow I_1$ (stretched exponential)			$I_1 \rightarrow I_2$ (exponential)		$I_2 \rightarrow I_2'$ (exponential)		$I_2' \rightarrow N$ (exponential)	
aging (h)	probe	A_0	A_1	β	k_1 ($\times 10^2$ s^{-1})	A_2	k_2 ($\times 10^4$ s^{-1})	A_3	k_3 ($\times 10^5$ s^{-1})	A_4	k_4 ($\times 10^6$ s^{-1})
3	far-UV CD	0.04	0.29(5)	0.93(16)	6.7(14)	0.30(1)	28(1)	0.25(6)	16(6)	0.12(5)	8.2(95)
	fluorescence	0.24	0.28(8)	0.48(9)	2.6(15)	0.26(3)	10(10)	0.19(2)	10(2)	0.11(2)	4.4(22)
	absorption	0.41	0.25(2)	0.35(3)	12(1)	0.092(5)	18(1)	0.12(2)	19(4)	0.097(15)	13(4)
4	far-UV CD	0.05	0.19(1)	1.5(2)	2.9(2)	0.34(1)	6.4(4)	0.22(2)	2.9(5)	0.2(11)	0.4(32)
	fluorescence	0.17	0.31(3)	0.51(4)	1.0(2)	0.24(2)	4.0(14)	0.08(11)	1.6(19)	0.08(8)	2.3(66)
	absorption	0.32	0.27(6)	0.23(5)	11(5)	0.17(1)	4.3(2)	0.12(2)	3.7(8)	0.08(1)	2.8(16)
16	far-UV CD	0.05	0.15(3)	0.68(12)	0.22(6)	0.40(21)	0.66(56)	0.18(3)	0.33(12)		
	fluorescence	0.14	0.32(3)	0.33(3)	0.65(14)	0.22(3)	0.83(26)	0.17(1)	0.49(5)		
	absorption	0.35	0.30(2)	0.22(1)	2.5(2)	0.16(1)	0.78(7)	0.12(2)	0.27(10)		
72	far-UV CD	0.07	0.15(9)	0.70(5)	0.0032(29)	0.40(5)	0.034(16)	0.25(95)	0.021(99)		
	fluorescence	0.12	0.31(19)	0.22(14)	0.17(11)	0.27(4)	0.038(18)	0.11(12)	0.040(65)		
	absorption	0.37	0.27(3)	0.17(2)	0.31(3)	0.17(1)	0.11(1)	0.21(16)	0.027(27)		

[a] Normalized time courses of changes in signals of far-UV CD at 222 nm, Trp59 fluorescence at 350 nm, and Soret absorption at 395 nm are fitted assuming a sequential pathway with four common intermediates ($U \rightarrow I_0 \rightarrow I_1 \rightarrow I_2 \rightarrow I_2' \rightarrow N$). A_0 is the amplitude of the initial unobservable burst phase of ~1 s, based on extrapolation of the signal to $t = 0$. The numbers in parentheses are the errors of the fitting parameters in the last, or the last two, digits.

folding to the more structured, molten globule intermediate, I_2', and (v) the final conformational readjustment step in the acquisition of the native structure, N. Although alternative mechanisms, such as an off-pathway mechanism, cannot be completely ruled out, a sequential scheme with four on-pathway intermediates (Scheme 1) seems more plausible, and it is consistent with the results obtained in aqueous solution (which will be discussed). We should note here that the observed folding process of cyt *c* in wet silica gels is almost reversible, in that the entrapped cyt *c*, after a single unfolding and refolding run, can reproducibly unfold and refold through the above-mentioned intermediates in the second cycle, although the second refolding kinetics tend to be slightly faster than the first ones especially when the first experimental run takes a long time to complete.

The folding began with the formation of I_0, characterized by a sharp change in the Soret absorption spectrum, which occurred in the initial unobservable burst phase of ~1 s. Within this burst phase ($U \rightarrow I_0$), the Soret band was red-shifted from ~395 to ~397 nm and its intensity was significantly decreased, resulting in 32−41% of the total change in absorption at 395 nm (Figure 2, green), while the characteristic high-spin charge-transfer marker band near 620 nm remained unchanged in intensity. These spectral features are consistent with the characteristics of a coordination change in the heme *c* group from a water-bound, five-coordinate state to a water−His18 bound six-coordinate state with an increase in pH from near 2 to above 4 (*30*). On the other hand, meanwhile, far-UV CD and Trp59 fluorescence exhibited only small changes that accounted for ~5 and 15−20% of the total, respectively (Table 1), indicating that the polypeptide chain is still in a nearly extended random conformation. Therefore, the major structural event occurring within the burst phase can be attributed to the deprotonation-induced His18 coordination to the heme iron.

Following the His18 ligation phase, the Trp59 fluorescence signal exhibited an initial kinetic phase leading to a collapsed intermediate I_1. This phase ($I_0 \rightarrow I_1$) was slow enough to be observed directly in all the samples (Figure 2A−D). During this phase, the fluorescence of Trp59 was quenched by ~50% from the initial level (Figure 2, red), but the CD signal at 222 nm reached only 20−30% of the native level (Figure 2, blue), indicating that I_1 adopts a partially collapsed conformation with a small amount of α-helix. Also meanwhile, the Soret band was gradually red-shifted from ~397 to ~399 nm and decreased in intensity to 59−66% from the initial level (Figure 2, green). Interestingly, as shown in Figure 1C, the fluorescence emission maximum of I_1 (~340 nm at 1.5 min) is significantly blue-shifted relative to that of U (~346 nm), suggesting the desolvation of Trp59 during the initial collapse.

The fluorescence-detected kinetics of this collapse phase ($I_0 \rightarrow I_1$) are nonexponential in time and can be well fit with stretched exponentials, $\exp[-(kt)^{\beta}]$, with stretching factors β ranging from 0.22 to 0.51; the β value decreases with an increase in the sol−gel aging time within the errors of estimation (Table 1). Stretched exponentials also account well for the corresponding absorbance- and CD-detected kinetics. However, the β values as well as the k values are different for the three probes. Regardless of the aging time, the stretching factor β is decreased in the following order: far-UV CD > Trp59 fluorescence > Soret absorption (Table 1).

The initial collapse phase was followed by two exponential phases leading to I_2 and I_2' (Figure 2A−D), characterized by a stepwise increase in helical content (far-UV CD) and a concurrent collapse (Trp59 fluorescence). Meanwhile, the Soret band is progressively red-shifted toward a more nativelike spectrum (Figure 1B). No significant probe dependence was found for the kinetics of these two exponential phases (Table 1). The data in Figures 1A and 2 (all panels) indicate that whereas I_2' has an 80% α-helical content (with respect to N) consistent with the general definition of the molten globule states (*31*), the α-helical content of I_2 is too low (60% with respect to N) to be considered a molten globular; hence, we refer it as a pre-molten globule intermediate. The existence of molten and pre-molten globule states are further supported by the following two observations. First, the Soret absorption spectra passed through two successive isosbestic points separated by ~1 nm (Figure 1B, inset). In addition, a charge-transfer band at 695 nm remained very small in the faster phase ($I_1 \rightarrow I_2$) but was markedly restored in the latter phase ($I_2 \rightarrow I_2'$) (Figure 1D), indicating a significant recovery of the iron−Met80 bond during the $I_2 \rightarrow I_2'$ process.

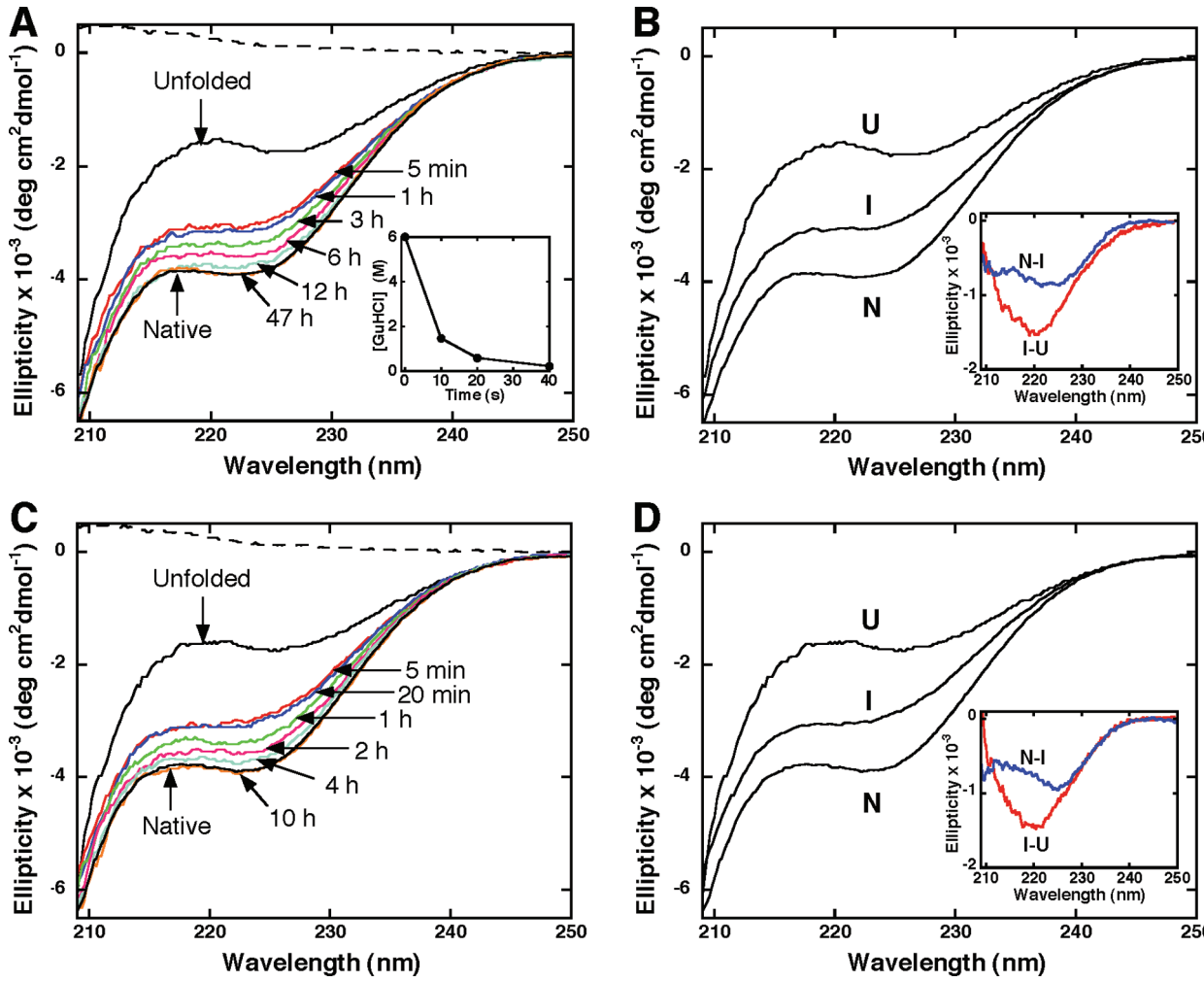

FIGURE 3: Transient far-UV CD spectra during the refolding of GuHCl-denatured ubiquitin at pH 5.0 (20 °C) in wet silica gels 0.1 mm in thickness. (A) Representative transient far-UV CD spectra of ubiquitin in the gel aged 96 h after a GuHCl concentration jump from 6.0 to 0 M. The dashed line is a baseline CD spectrum of a wet silica gel without protein. Times indicated are those after reduction of the concentration of GuHCl to <0.58 M. The inset shows the decay of the GuHCl concentration inside the protein-free 0.1 mm silica gel sheet (monitored by the absorbance at 207.5 nm) after the bathing buffer had been changed from one that contains 6.0 M GuHCl to one that contains no GuHCl. (B) Comparison of the best-fit CD spectra for U, I, and N that appear during the refolding of ubiquitin in the gel aged 96 h. The transient CD spectra at 15 time points (including $t = 0$) were globally fit to a three-state model (U → I → N). The inset shows difference spectra between each species. (C) Representative transient far-UV CD spectra of ubiquitin in the gel aged 16 h after a GuHCl concentration jump from 6.0 to 0 M. The dashed line is a baseline CD spectrum of a wet silica gel without protein. Times indicated are those after reduction of the concentration of GuHCl to <0.58 M. (D) Comparison of the best-fit CD spectra for U, I, and N that appear during the refolding of ubiquitin in the gel aged 16 h. The transient CD spectra at 11 time points (including $t = 0$) were globally fit to a three-state model (U → I → N). The inset shows difference spectra between each species.

Finally, the remaining changes for all conformational probes occurred in a minor adjustment phase on a much slower time scale. This adjustment phase ($I_2' \rightarrow N$) is fully and partly seen in panels A and B of Figure 2, respectively, while not seen in panels C and D of Figure 2 because of its extreme slowness. Representative transient CD, Soret absorption, Trp fluorescence, and charge-transfer band absorption spectra for the sample aged for 3 h confirm that cyt *c* almost reaches the native state at the end of this phase (Figure 1E−H). It is generally believed that at least part of this adjustment phase reflects some nonobligatory barrier, such as a wrong proline isomer (*19*).

Ubiquitin Unfolding and Refolding. For ubiquitin experiments, we used three samples with aging times of 16, 48, and 96 h. Each aged sample was initially unfolded by immersion in buffer (0.05 M potassium phosphate at pH 5.0) containing 6.0 M GuHCl at 20 °C, and refolding was triggered by changing the bathing buffer to one that contains no GuHCl at 20 °C. Regardless of the aging time, the CD spectra of the native (N) and unfolded (U) states of ubiquitin (Figure 3A,C) are qualitatively similar to the corresponding solution spectra as reported previously (*21*). It is important to note that the time required for reducing the GuHCl concentration inside the silica gels is sufficiently short to enable monitoring of the refolding of ubiquitin in silica gels on the basis of far-UV CD measurements (Figure 3A, inset; see also details in Experimental Procedures).

Figure 4 shows the refolding kinetics of ubiquitin in silica gels aged for 16, 48, and 96 h. No significant CD changes were observed within the dead time of the measurements (i.e., ~1 s when using silica gels ~0.02 mm in thickness). All the samples appear to exhibit two distinct exponential phases: (i) a fast phase with a time constant of approximately 20 s, which accounts for 60−65% of total CD change observed at 222 nm, and (ii) a slower phase with a time constant of hours depending on the aging time, which

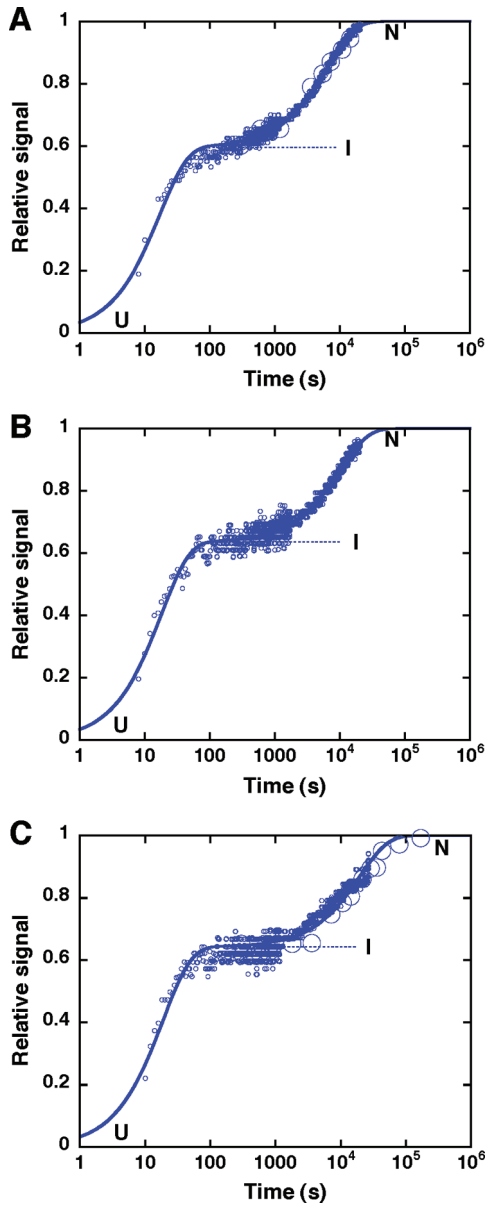

FIGURE 4: Normalized time courses of changes in signals of far-UV CD at 222 nm during the refolding of GuHCl-denatured ubiquitin at pH 5.0 (20 °C) in wet silica gels aged for (A) 16, (B) 48, and (C) 96 h, plotted on a logarithmic time scale. Refolding was triggered by changing the bathing buffer from one that contains 6.0 M GuHCl to one that contains no GuHCl. In each panel, the data obtained from ~0.02 mm silica gel samples are shown as small empty circles. Solid lines are the best fits of these data to a double-exponential function. Dotted lines indicate the faster exponential component to form I. In panels A and C, the corresponding data obtained from 0.1 mm silica gel samples (large empty circles; calculated from the spectral data shown in Figure 3) are plotted for comparison.

accounts for the remaining 35−40% of the CD change. Clearly, these kinetic data are much simpler than those of cyt *c* (shown in Figure 2). The data also suggest that an intermediate state (I) is populated during the refolding of ubiquitin in wet silica gels, which is in marked contrast to the apparent two-state folding kinetics observed in solution CD studies (*21*).

To further characterize this intermediate I, the transient CD spectra during the refolding of ubiquitin in 0.1 mm silica gels aged for 96 and 16 h (shown in panels A and C of Figure 3, respectively) were globally fit to a three-state model (U → I → N). The best-fit CD spectra for U, I, and N are shown in panels B and D of Figure 3, along with difference spectra between each species. Similar results were obtained for the samples aged for both 96 and 16 h, although the slow phase rates are different (Table 2). Significantly, the difference spectrum between U and I differs in shape from that between I and N: the former mainly reflects the α-helix formation characterized by the negative CD around 220 nm, whereas the latter includes both formation of the α-helix and formation of β-sheet structure characterized by the negative CD band in the 210−215 nm region (Figure 3B,D, insets). Thus, these data provide evidence of the occurrence of an intermediate with at least partially formed α-helix, followed by a slow propagation process during which the native β-strand and the entire α-helix are formed.

Table 2: Kinetic Parameters for the Refolding Kinetics of GuHCl-Denatured Ubiquitin at pH 5.0 (20 °C) in Wet Silica Gels Aged for 16, 48, and 96 h on the Basis of CD Measurements at 222 nm[a]

	U → I		I → N	
aging (h)	A_{fast}	k_{fast} ($\times 10^2$ s^{-1})	A_{slow}	k_{slow} ($\times 10^4$ s^{-1})
16	0.60(1)	5.9(1)	0.40(1)	1.6(1)
	−	1.7(21)[b]	−	1.4(1)[b]
48	0.63(2)	5.5(2)	0.37(2)	1.0(1)
96	0.64(3)	5.3(3)	0.36(1)	0.51(2)
	−	1.6(12)[b]	−	0.43(3)[b]

[a] The parameters are estimated from double-exponential fitting on the kinetic data shown in Figure 4. The numbers in parentheses are the errors of the fitting parameters in the last, or the last two, digits. [b] Estimated from the global analysis. The transient CD spectra shown in Figure 3 are globally fit to a three-state model (U → I → N).

DISCUSSION

These results demonstrate that entrapment of cyt *c* in wet, optically transparent, porous silica gel matrices allows slow motion analysis of the rapid folding events with a combination of spectroscopic techniques. Compared to cyt *c* refolding in aqueous solution, the deceleration factor is 10^5-10^9 depending on the sol−gel aging time (Figure 2). A similar deceleration effect was also seen in the smaller protein ubiquitin, which folds with a time constant of approximately 10 ms in aqueous solution at 20 °C (*21*). These observations are somewhat surprising, in view of the fact that the protein molecule in aged wet silica gels is surrounded by many water molecules, which make up more than the total gel volume (a water mass fraction of 70%). Although the physical basis of this deceleration effect is not fully understood, recent experimental results highlight an indirect mechanism in which the gel matrix could influence the protein dynamics by affecting the dynamics of the surrounding solvent (*10*). This indirect effect is probable, because protein motions are intimately linked to the motions of the environment (*32*), and because water in nanoscopic environments is known to have a decreased solvent dynamics compared to bulk water (*10, 33*). It is reasonably assumed that fine pore networks of aged wet silica gels [typically 50−100 Å (*5*)] could confine a nanoscopic layer of water around protein surface, which in turn impedes large-scale protein motions. It should also be noted that large-scale protein motions proceed in a large number of elementary steps, each controlled by the solvent fluctuations, and thus can be slowed by a large factor.

It is also possible that the silanol group (Si-OH) on the silica pore walls could make hydrogen bonding or electrostatic interactions directly with the surface of the protein. However, we believe that these direct interactions are not likely to be the major cause of the deceleration effect, because of the following reasons. First, previous studies on human adult hemoglobin (pI ~7.0) show that, despite its neutrality at pH 7.0, the gel entrapment (pH 7.0) causes its quaternary structural change to decelerate by a factor of 10^{10} (*7*). Second, a recent NMR study demonstrates that the gel entrapment (pH 7.0) causes an only 2-fold increase in the average rotational correlation time for sperm whale myoglobin (pI ~7.5), implying that the entrapping cage still has some free space (*34*). Nevertheless, the gel entrapment of myoglobin (pH 7.0) dramatically slows its ligation-linked conformational change by a factor of 10^7 (*9*), supporting the relative importance of indirect interactions as compared to direct interactions at least in the case of myoglobin. In the same study (*34*), the average rotational correlation time for cyt *c* (pI ~9.5) in wet silica gels (pH 8.0) cannot be determined from its NMR resonances that are too broadened, presumably by electrostatic interactions between cyt *c* and gel matrix, to be analyzed. However, dipolar relaxation measurement of cyt *c* in silica gel thin films (pH 4.25) shows that the gel matrix restricts the rotational motion of cyt *c* only to a small extent (~1.1 kcal/mol), indicating that there should be water between even cationic cyt *c* and the gel matrix (*35*). We therefore speculate that nonspecific long-range electrostatic interactions between cyt *c* and the gel matrix, together with water-mediated indirect interactions, contribute to the deceleration effect seen in the case of cyt *c* folding.

Although the folding time of cyt *c* in wet silica gels is very different from that in aqueous solution, it is notable that the overall folding pathways appear to be similar in these two environments. Our proposed scheme for cyt *c* refolding in silica gels ($U \rightarrow I_0 \rightarrow I_1 \rightarrow I_2 \rightarrow I_2' \rightarrow N$) is, in fact, in general agreement with solution phase data that indicate that a sequential scheme with two intermediates ($U \rightarrow I_C \rightarrow I_M \rightarrow N$, where I_C and I_M represent the collapsed and molten globule intermediates, respectively) is the simplest mechanism for explaining cyt *c* folding under conditions similar to those used here (*15, 16, 19*). The early collapsed intermediate I_C (formed within 100 μs in solution) is similar to I_1 in silica gels, in that both exhibit a 50−60% reduction in the Trp59 fluorescence intensity compared to that of U (*15, 19*) and have only a small amount (~20%) of native helical structure (*16*). Likewise, the molten globule intermediate I_M may correspond to I_2' in silica gels, because they are very similar in far-UV CD spectra and in Trp59 fluorescence intensity (80−90% reduction from the initial level). Moreover, our observation that the Met80−iron bond is significantly restored in I_2' is in agreement with resonance Raman measurements, showing that ~50% of the Met80−iron bond is generated within 1 ms (*19*), at which time I_M accumulates under the same refolding conditions (*16*). Thus, the folding intermediates populated in solution and in gel environments share structural similarity pointing to a common folding pathway.

Note, however, that earlier stopped-flow studies show that the recovery of absorption at 695 nm occurs more slowly with an ~15 ms time constant at pH 4.9 (*36, 37*). This observation suggests that the Met80 coordination is associated with the formation step of N, which is clearly inconsistent with the results given above. The exact cause of this discrepancy is unclear but could result from the presence of 0.7−1.5 M guanidine hydrochloride in the refolding solution of those studies (*36, 37*). Shastry and Roder pointed out that the amplitudes of the submillisecond folding phases decrease sharply with an increase in guanidine hydrochloride concentration (*15*). Thus, it is possible that, in the presence of the denaturant, the final process gains amplitude at the expense of the faster phases, which makes the folding process an apparent two-state transition, as reported previously (*36, 37*).

Our results also reveal two previously undetected intermediates, I_0 and I_2. The former is the precollapsed intermediate with His18 bound to the heme, and the latter is the pre-molten globule intermediate still lacking the Fe−Met80 bond. In solution, the coordination of His18 to the heme iron occurs concurrent with chain collapse during the nascent phase (*38*). By contrast, in silica gels, these two processes become decoupled (Figure 2A−D). This kinetic decoupling can be explained as follows. In silica gels, the larger-scale protein motion may be more hindered by the confinement of the surrounding water. Therefore, the local protein motions for His18 binding to the heme iron are separated from the global collapse. Since His18 is right next to the thioether linkage between the heme and the polypeptide chain, this conformational constraint allows His18 to bind to the heme iron even in the nearly extended conformation of I_0. On the other hand, the Met80 binding to the heme iron ($I_2 \rightarrow I_2'$) is postponed until the formation of pre-molten globule state I_2. This may be because this bond formation needs a nativelike topology of the chain that makes Met80 (on the loop of residues 70−85) accessible to the heme iron.

The results presented above suggest an interesting possibility that our approach is able to stabilize and capture on-pathway "hidden" folding intermediates (such as I_0 and I_2) that may exist on the folding pathway but escape detection by conventional techniques. This possibility is also in agreement with our data showing that a normally unstable partially structured intermediate I is populated during ubiquitin folding when entrapped in wet silica gels (Figures 3 and 4). It should be mentioned here that the observed α-helix-rich ubiquitin intermediate is not likely to result from the microscopic heterogeneity of the gel environment, because it is highly unlikely that the spectral sum of the two spectrally distinct components, if originating from two environments, is coincidentally similar to the native CD spectrum. Moreover, low-temperature stopped-flow experiments with ubiquitin mutants under high-viscosity conditions support the rapid formation of an α-helix-rich folding intermediate (*26*). During the refolding of a double mutant ubiquitin (F45W/I61A) in the presence of 45% ethylene glycol, a very large burst phase has been observed at −20 °C by detection of changes in CD at 222 nm (*26*). The formation of this intermediate and the acquisition of nativelike fluorescence were separated by a factor of >500 in time. Consistent with this, our data show that the native CD signature is acquired at least 100 times more slowly than the formation of the α-helix-rich intermediate (Figure 4 and Table 2), indicating that the initial helix formation occurs long before the acquisition of the native structure.

It is very important to point out that attempts to vary the strength of the gel network by varying the sol−gel aging time are found to have a dramatic effect on the folding time, but no measurable effect on the structural features of the four above-mentioned intermediates of cyt *c* (Figure 2). The same situation holds in the case of ubiquitin (Figure 4), although the effect on the folding time is not as dramatic as that observed for cyt *c*. These findings provide strong support for the argument that the interaction between the protein and gel matrix has no measurable effect on the overall folding pathway in silica gels. This finding also implies that microscopic heterogeneity of the gel interior, if any, does not complicate the folding pathway and thus not alter the main conclusions drawn in this study.

However, the situation becomes more complex when we consider the kinetics of cyt *c* folding. Our data indicate that the early folding kinetics of cyt *c* in silica gels ($I_0 \rightarrow I_1$) exhibit a stretched exponential character and probe dependence (Figure 2A−D and Table 1) while the later phases ($I_1 \rightarrow I_2$ and $I_2 \rightarrow I_2'$) show nearly probe-independent exponential kinetics. This is in contrast to the previous solution studies showing that the early collapse of cyt *c* exhibits an exponential fluorescence decay (*15, 17*). The single-exponential kinetics are explained by a two-state barrier crossing process. By contrast, the stretched exponential kinetics are explained by a transition state ensemble, possibly resulting from glass transition (*18, 39*) or the heterogeneous microenvironment of each chain. Within this scenario, the strong probe dependence could be ascribed to a multiphased collapse of the individual chains within silica gel matrices, causing the accumulation of many intermediates on parallel pathways between I_0 and I_1. An alternative and more interesting possibility is that the early collapse in silica gels is a downhill process without significant free energy barriers (*39–42*). Such mechanistic switching from barrier-limited to barrierless folding may occur at the disappearance of an entropic barrier, as the level of restriction imposed by the gel matrix increases. Unfortunately, our data do not allow us to distinguish these two possibilities. However, in either case, the results do suggest the potential usefulness of our method for separation of a large number of intermediate structures between I_0 and I_1.

In conclusion, the results for cyt *c* refolding in wet silica gels reveal a sequence of four distinct intermediates with progressively increasing degrees of folding. Independent solution experiments replicate some of the specific steps in the proposed pathway (*16*). Moreover, our additional studies on a simple model protein ubiquitin illustrate the ability of our approach to stabilize and capture normally unstable high-energy intermediates. The results demonstrated here open the way to identifying a sequence of folding events that likely occurs but has been only partly observed in solution experiments.

ACKNOWLEDGMENT

I thank Dr. Satoshi Saigo and Dr. Shuji Akiyama for helpful discussions and comments.

REFERENCES

1. Eaton, W. A., Muñoz, V., Hagen, S. J., Jas, G. S., Lapidus, L. J., Henry, E. R., and Hofrichter, J. (2000) Fast kinetics and mechanisms in protein folding. *Annu. Rev. Biophys. Biomol. Struct. 29*, 327–359.
2. Ballew, R. M., Sabelko, J., and Gruebele, M. (1996) Direct observation of fast protein folding: The initial collapse of apomyoglobin. *Proc. Natl. Acad. Sci. U.S.A. 93*, 5759–5764.
3. Jones, C. M., Henry, E. R., Hu, Y., Chan, C.-K., Luck, S. D., Bhuyan, A., Roder, H., Hofrichter, J., and Eaton, W. A. (1993) Fast events in protein folding initiated by nanosecond laser photolysis. *Proc. Natl. Acad. Sci. U.S.A. 90*, 11860–11864.
4. Chen, R. P.-Y., Huang, J. J.-T., Chen, H.-L., Jan, H., Velusamy, M., Lee, C.-T., Fann, W., Larsen, R. W., and Chan, S. I. (2004) Measuring the refolding of β-sheets with different turn sequences on a nanosecond time scale. *Proc. Natl. Acad. Sci. U.S.A. 101*, 7305–7310.
5. Ellerby, L. M., Nishida, C. R., Nishida, F., Yamanaka, S. A., Dunn, B., Valentine, J. S., and Zink, J. I. (1992) Encapsulation of proteins in transparent porous silicate glasses prepared by the sol-gel method. *Science 255*, 1113–1115.
6. Shibayama, N., and Saigo, S. (1995) Fixation of the quaternary structures of human adult haemoglobin by encapsulation in transparent porous silica gels. *J. Mol. Biol. 251*, 203–209.
7. Shibayama, N., and Saigo, S. (1999) Kinetics of the allosteric transition in hemoglobin within silicate sol-gels. *J. Am. Chem. Soc. 121*, 444–445.
8. Shibayama, N. (1999) Functional analysis of hemoglobin molecules locked in doubly liganded conformations. *J. Mol. Biol. 285*, 1383–1388.
9. Shibayama, N., and Saigo, S. (2003) Oxygen equilibrium properties of myoglobin locked in the liganded and unliganded conformations. *J. Am. Chem. Soc. 125*, 3780–3783.
10. Massari, A. M., Finkelstein, I. J., and Fayer, M. D. (2006) Dynamics of proteins encapsulated in silica sol-gel glasses studied with IR vibrational echo spectroscopy. *J. Am. Chem. Soc. 128*, 3990–3997.
11. Samuni, U., Navati, M. S., Juszczak, L. J., Dantsker, D., Yang, M., and Friedman, J. M. (2000) Unfolding and refolding of sol-gel encapsulated carbonmonoxymyoglobin: An orchestrated spectroscopic study of intermediates and kinetics. *J. Phys. Chem. B 104*, 10802–10813.
12. Navati, M. S., Samuni, U., Aisen, P., and Friedman, J. M. (2003) Binding and release of iron by gel-encapsulated human transferrin: Evidence for a conformational search. *Proc. Natl. Acad. Sci. U.S.A. 100*, 3832–3837.
13. Viappiani, C., Bettati, S., Bruno, S., Ronda, L., Abbruzzetti, S., Mozzarelli, A., and Eaton, W. A. (2004) New insights into allosteric mechanisms from trapping unstable protein conformations in silica gels. *Proc. Natl. Acad. Sci. U.S.A. 101*, 14414–14419.
14. Elöve, G. A., Chaffotte, A. F., Roder, H., and Goldberg, M. E. (1992) Early steps in cytochrome c folding probed by time-resolved circular dichroism and fluorescence spectroscopy. *Biochemistry 31*, 6876–6883.
15. Shastry, M. C. R., and Roder, H. (1998) Evidence for barrier-limited protein folding kinetics on the microsecond time scale. *Nat. Struct. Biol. 5*, 385–392.
16. Akiyama, S., Takahashi, S., Ishimori, K., and Morishima, I. (2000) Stepwise formation of α-helices during cytochrome c folding. *Nat. Struct. Biol. 7*, 514–520.
17. Hagen, S. J., and Eaton, W. A. (2000) Two-state expansion and collapse of a polypeptide. *J. Mol. Biol. 301*, 1019–1027.
18. Saigo, S., and Shibayama, N. (2003) Highly nonexponential kinetics in the early-phase refolding of proteins at low temperatures. *Biochemistry 42*, 9669–9676.
19. Zhong, S., Rousseau, D. L., and Yeh, S.-R. (2004) Modulation of the folding energy landscape of cytochrome c with salt. *J. Am. Chem. Soc. 126*, 13934–13935.
20. Babul, J., and Stellwagen, E. (1972) Participation of the protein ligands in the folding of cytochrome c. *Biochemistry 11*, 1195–1200.
21. Gladwin, S. T., and Evans, P. A. (1996) Structure of very early protein folding intermediates: New insights through a variant of hydrogen exchange labeling. *Folding Des. 1*, 407–417.
22. Krantz, B. A., and Sosnick, T. R. (2000) Distinguishing between two-state and three-state models for ubiquitin folding. *Biochemistry 39*, 11696–11701.
23. Went, H. M., Benitez-Cardoza, C. G., and Jackson, S. E. (2004) Is an intermediate state populated on the folding pathway of ubiquitin? *FEBS Lett. 567*, 333–338.
24. Vijay-Kumar, S., Bugg, C. E., and Cook, W. J. (1987) Structure of ubiquitin refined at 1.8 Å resolution. *J. Mol. Biol. 194*, 531–544.

25. Khorasanizadeh, S., Peters, I. D., and Roder, H. (1996) Evidence for a three-state model of protein folding from kinetic analysis of ubiquitin variants with altered core residues. *Nat. Struct. Biol. 3*, 193–205.
26. Larios, E., Li, J. S., Schulten, K., Kihara, H., and Gruebele, M. (2004) Multiple probes reveal a native-like intermediate during low-temperature refolding of ubiquitin. *J. Mol. Biol. 340*, 115–125.
27. Tsong, T. Y. (1976) Ferricytochrome c chain folding measured by the energy transfer of tryptophan 59 to the heme group. *Biochemistry 15*, 5467–5473.
28. Brinker, C. J., and Scherer, G. W. (1990) *Sol-Gel Science: The Physics and Chemistry of Sol-Gel Processing*, Academic Press, San Diego.
29. Droghetti, E., and Smulevich, G. (2005) Effect of sol-gel encapsulation on the unfolding of ferric horse heart cytochrome c. *J. Biol. Inorg. Chem. 10*, 696–703.
30. Hirota, S., Suzuki, M., and Watanabe, Y. (2004) Hydrophobic effect of trityrosine on heme ligand exchange during folding of cytochrome c. *Biochem. Biophys. Res. Commun. 314*, 452–458.
31. Kuwajima, K. (1989) The molten globule state as a clue for understanding the folding and cooperativity of globular-protein structure. *Proteins: Struct., Funct., Genet. 6*, 87–103.
32. Frauenfelder, F., Fenimore, P. W., Chen, G., and McMahon, B. H. (2006) Protein folding is slaved to solvent motions. *Proc. Natl. Acad. Sci. U.S.A. 103*, 15469–15472.
33. Levinger, N. E. (2002) Water in confinement. *Science 298*, 1722–1723.
34. Wheeler, K. E., Nocek, J. M., and Hoffman, B. M. (2006) NMR spectroscopy can characterize proteins encapsulated in a sol-gel matrix. *J. Am. Chem. Soc. 128*, 14782–14783.
35. Dave, B. C., Soyez, H., Miller, J. M., Dunn, B., Valentine, J. S., and Zink, J. I. (1995) Synthesis of prtein-doped sol-gel SiO_2 thin films: Evidence for rotational mobility of encapsulated cytochrome c. *Chem. Mater. 7*, 1431–1434.
36. Sosnick, T. R., Mayne, L., Hiller, R., and Englander, S. W. (1994) The barriers in protein folding. *Nat. Struct. Biol. 1*, 149–156.
37. Sosnick, T. R., Mayne, L., and Englander, S. W. (1996) Molecular collapse: The rate-limiting step in two-state cytochrome c folding. *Proteins: Struct., Funct., Genet. 24*, 413–426.
38. Roder, H., Maki, K., Latypov, R. F., Cheng, H., and Shastry, M. C. R. (2005) *Protein Folding Handbook, Part I*, pp 491−535, Wiley-VCH, Weinheim, Germany.
39. Socci, N. D., Onuchic, J. N., and Wolynes, P. G. (1998) Protein folding mechanisms and the multidimensional folding funnel. *Proteins: Struct., Funct., Genet. 32*, 136–158.
40. Bryngelson, J. D., Onuchic, J. N., Socci, N. D., and Wolynes, P. G. (1995) Funnels, pathways, and the energy landscape of protein folding: A synthesis. *Proteins: Struct., Funct., Genet. 21*, 167–195.
41. Sabelko, J., Ervin, J., and Gruebele, M. (1999) Observation of strange kinetics in protein folding. *Proc. Natl. Acad. Sci. U.S.A. 96*, 6031–6036.
42. Ma, H., and Gruebele, M. (2005) Kinetics are probe-dependent during downhill folding of an engineered λ_{6-85} protein. *Proc. Natl. Acad. Sci. U.S.A. 102*, 2283–2287.

BI8003582